Available online at www.sciencedirect.com
SCIENCE DIRECT
Polymer 47 (2006) 3477–3485
polymer
www.elsevier.com/locate/polymer

Molecular mobility of crosslinked elastomers stretched above T_g

E. Munch *, J.M. Pelletier, B. Sixou, G. Vigier

GEMPPM, UMR CNRS 5510, INSA de Lyon, 69621 Villeurbanne Cedex, France

Received 11 January 2006; received in revised form 16 February 2006; accepted 13 March 2006
Available online 3 April 2006

Abstract

A uniaxial deformation is performed on a styrene–butadiene elastomer and two nitril butadiene elastomers with two different crosslinking densities in their rubbery state. The slow α-relaxation process is investigated under constant deformation using low frequency dynamic mechanical analysis. No effect is observed in the stretched elastomers although microstructural changes are detected thanks to tensile tests and wide angle X-ray scattering experiments. A possible explanation of these results is that the inter-molecular interactions are not significantly modified in the stretched network.

Keywords: Crosslinked thermoplastic elastomers; Molecular mobility; Uniaxial extension

1. Introduction

It is generally accepted that molecular mobility is an important factor in determining the macroscopic mechanical properties of glass-forming systems like polymers but a comprehensive knowledge of the effect of the molecular motions on the mechanical behavior is not yet achieved. This understanding should rely on a model of deformation processes at the molecular scale. A comprehension of the relation between molecular mobility and local polymer structure should bring insights in understanding phenomena like the reinforcement at large deformations in amorphous polymer, or the modification of the local mobility around the fillers induced by deformation in composite materials.

Different types of motions are taking place in polymers at various time and length scales depending on temperature. Fast processes corresponding to the nanometer range are usually observed via quasi-elastic neutron scattering or low frequency Raman scattering measurements [1]. Localized motions are responsible for the secondary relaxations while the α process is associated with cooperative motions of larger scale. This relaxation is associated to the glass transition temperature [2]. The Rouse modes and reptation determine the mobility for longer time scales and larger length scales [3].

All these motions are affected by the nature of chain, the flexibility of the chain backbone, the steric hindrance of pendant groups and the structural state of the polymer. These parameters modify the relaxation processes and the interactions between neighboring bonded and non-bonded segments [3]. The effect of the microstructural state of the polymer on mobility has been already studied. The microstructure can be modified according to different procedures like annealing, physical ageing or plastic deformation. As pointed out by Oleynik, the deformation mechanisms may be completely different when the deformation is carried out above or below T_g [4].

Among theories, which describe the behavior of amorphous materials around their glass temperature transition, the free volume theory relates the visco-elastic events to time and temperature, gives a relation between the coefficients of expansion above T_g, but poorly describes the motions at a molecular level. This theory is applicable above T_g but is often used in an improper manner below. The kinetic theories describe quantitatively the shifts in T_g with time, determines the heat capacities, but do not predict T_g at infinite time scales. The thermodynamic theory predicts the variations of T_g with molecular weight, crosslinking density, predicts a transition temperature but poorly defines it [5].

When one considers the impact of deformation on the microstructure, a clear distinction has to be made between the macroscopic approach of the thermodynamic models, which evaluate the energetic and entropic contributions to the stress, and the local approach of the models, which study the variation of mobility as a function of entropy and energy of activation.

* Corresponding author. Tel.: +33 472 43 6357; fax: +33 472 43 8528.
E-mail address: etienne.munch@insa-lyon.fr (E. Munch).

0032-3861/$ - see front matter © 2006 Elsevier Ltd. All rights reserved.
doi:10.1016/j.polymer.2006.03.043

The global models calculate a variation of internal energy and entropy in a thermodynamic transformation from a non-deformed state to a deformed one. The thermo-mechanical behavior of elastomers has been the subject of many investigations through non-trivial thermo-elastic measurements [6–8], which attempt to correlate the stress or the strain to variations of entropy and more rarely of enthalpy. But no information on the mobility can be extracted from these considerations.

In some calorimetric measurements on elastomers under uniaxial extension, a competition has been shown between an increase in vibration entropy connected with the volume change with deformation and a decrease in conformational entropy connected with the change of shape with deformation. It must be emphasized that in all case, the volume changes remain always weak because of the incompressibility of the material. In this study, Frosini et al. [9] made a calculation of the variation of internal energy during a thermodynamic transformation, disconnected from molecular mobility. They made use of the general equation of state for the Gaussian polymer network resolving the total elastic force into energetic and entropic components. It has been demonstrated that the energy contribution is practically independent of extension ratio.

In addition to thermodynamic considerations, one has to consider the variations of the mobility as a function of activation entropy and activation energy parameters such as in the Starkweather formalism [10,11]. The model starts from the theory of absolute reaction rate, which appears to be equivalent to an Arrhenius function

$$f = \frac{kT}{2\pi h}\exp\left(\frac{\Delta S_a}{k}\right)\exp\left(-\frac{\Delta H_a}{kT}\right)$$

where, ΔH_a is the activation enthalpy; ΔS_a the activation entropy; T the temperature; k the Boltzmann constant; h the Planck constant.

On the base of this formulation, we are going to test whether or not the deformation has an impact on ΔS_a and ΔH_a.

Only a few studies have investigated the effects of a deformation on mobility. Diaz Calleja and co-workers in an attempt to test if the free volume theory holds for elongated networks, observed a shift of the main α transition associated loss factor peak with elongation for amorphous networks [12,13]. The use of the compensation law as well as the free volume theory appeared to be valid and they considered their observations to be the result of two competitive and opposite effects, the increase in free volume and a decrease in conformational entropy caused by static strain. They finally stated that the increase in the activation entropy with increasing static strain is consistent with a decrease in the conformational entropy with orientation of the chain.

In order to shed light on these points, amorphous crosslinked elastomers are deformed at temperatures above their respective glass transition temperatures (T_g) and then cooled down to the glassy state under constant deformation.

Two different elastomers, a styrene–butadiene rubber (SBR) and a nitril–butadiene rubber (NBR) are studied in order to check the effect of the molecular structure. The NBR undergoes a thermal treatment in order to test the impact of a variation of the reticulation ratio.

The first part of the work concerns the characterization of the materials in a non-deformed state. Then, tensile tests are performed to determine the response of the materials to a uniaxial deformation. Finally, we study the effect of deformation on the conformational entropy, on the microstructure and at last on molecular mobility.

2. Experimental

Styrene–butadiene (SBR) and nitril–butadiene rubbers (NBR) are thermoplastic elastomers, which do not crystallize under deformation with a glass transition temperature T_g around 263 and 243 K, respectively. The synthetic rubbers used in this work are statistic copolymers made up of 1,2-butadiene (55%), 1,4-butadiene (20%), and styrene (25%) for SBR (density of 1.031 g cm^{-3}) and of butadiene (72%) and acrylo-nitril (28%) for NBR (density of 1.034 g cm^{-3}). The NBR initially weakly vulcanized, is subjected to an annealing treatment (2 h at 403 K) in order to modify its crosslinking density. The dynamic mechanical analysis (DMA) is carried out with a torsion pendulum developed in our laboratory [14]. The original device is modified in order to be able to maintain a constant deformation to the samples during the test (Fig. 1).

The dead weight that usually compensates the weight of the sample and the assembly to insure a pure torsion testing is replaced by a laboratory lift fixed to the ground of the apparatus, which allows us to vary the length of our sample. All the samples were in an equilibrium state before cooling below T_g with a cooling rate of 3°/min approximately. The isochronal DMA experiments are realized at 1 Hz, with a rate of 1°/min starting from 90 K up to above T_g (Fig. 2).

For the construction of the master curves, a temperature ramp by steps of 2° is imposed, and the complex modulus is measured at each temperature step for frequencies varying

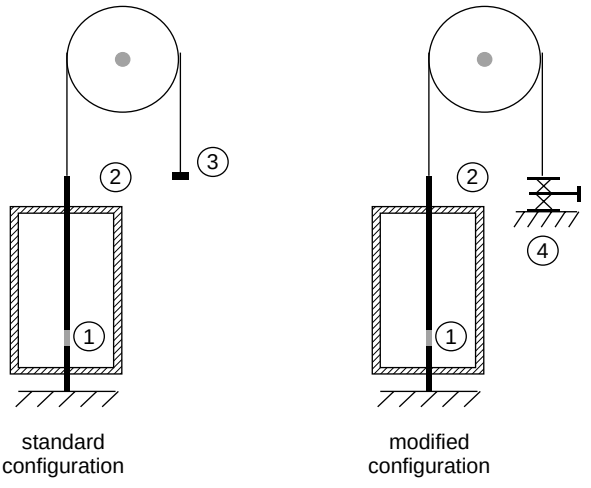

Fig. 1. Scheme of the modified torsion pendulum apparatus: where, (1) is the sample; (2) is the regulation temperature system; (3) is the dead weight and (4) is the elongation regulation system.

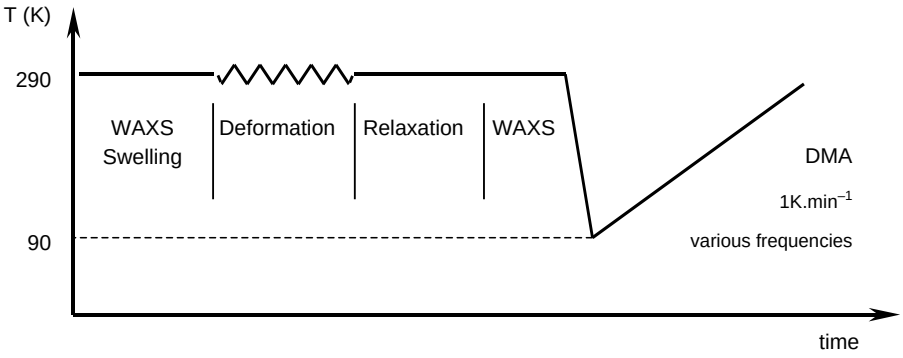

Fig. 2. Scheme of the experimental procedure.

from 3.10^{-2} to 3 Hz. The mechanical behavior in tension of the material is obtained with a tensile device MTS at room temperature and at a strain rate of $0.4\ s^{-1}$. The swelling measurements are done in dichloromethane, whose density is $1.325\ g\ cm^{-3}$, and which presents interaction parameters χ of 0.47 and 0.31 with SBR and NBR, respectively [15].

The X-ray measurements were carried out with a wavelength of 1.54 Å. The two-dimensional WAXS patterns were recorded using a Princeton Instrument PI-SCX ccd camera and the images were processed using the associated software 'winview'.

3. Results

3.1. Microstructural characterization of non-deformed materials

3.1.1. Network characterization by swelling

The results of swelling measurements are presented in Table 1. The determination of the density of active chains is done on the base of the Flory–Rehner Eq. (1), which considers that the positive entropy change arises from mixing polymer and solvent, and that the negative entropy change is caused by the reduction of the number of the possible chain conformations and by the heat of mixing polymer and solvent [15,16].

$$-[\ln(1-v_2)+v_2+\chi v_2^2] = Vn\left[v_2^{1/3}-\frac{v_2}{2}\right] \quad (1)$$

where, v_2 is the volume fraction of the polymer in the swollen mass; V is the molar volume of solvent; χ is the Flory–Huggins interaction parameter and n is the density of active chains.

In the as received state SBR and NBR present two different molecular masses between crosslinks, difference that is enhanced by the annealing treatment, which leads to an increase in the density of active chains between crosslinks.

Table 1
Results obtained for swelling experiments of SBR and NBR in dichloromethane

Material	χ		Density of active chains (mol cm^{-3})	Average number of monomers between crosslinks
SBR	0.47	As received	9.18×10^{-5}	235
NBR	0.31	As received	1.80×10^{-4}	103
NBR	0.31	Annealed	2.09×10^{-4}	88

3.1.2. Deformation of the materials and influence on entropy

The purpose of these experiments is to determine the deformation ratios that can be reached with our materials and the impact that the deformation has on the conformational entropy. The mechanical behavior under uniaxial deformation is presented on Fig. 3, which displays the evolution of the nominal stress versus nominal strain, for SBR and NBR as received and annealed. The mechanical results confirm the lower density of crosslinks in the SBR, which presents a lower value of modulus. The annealing treatment appears to increase the modulus of the NBR and to reduce its elongation at break.

The theory of the rubber elasticity may be useful to understand the effects of a macroscopic deformation on the local arrangement of macromolecules. In the framework of the classical theory of rubber elasticity, the deformation behavior of an ideal network of Gaussian chains is given by [17]

$$\sigma = \frac{\rho RT}{M_c}(\lambda^2-\lambda^{-1})$$

where, $\lambda = l/l_0$ is the uniaxial stretch ratio; l is the sample length after elongation; l_0 is the initial sample length; σ is the nominal stress (MPa); ρ is the density of the elastomer ($g\ cm^{-3}$); M_c is the molar mass between crosslinking points ($g\ mol^{-1}$); T is the temperature (K) and R is the gas constant ($J\ K^{-1}\ mol^{-1}$).

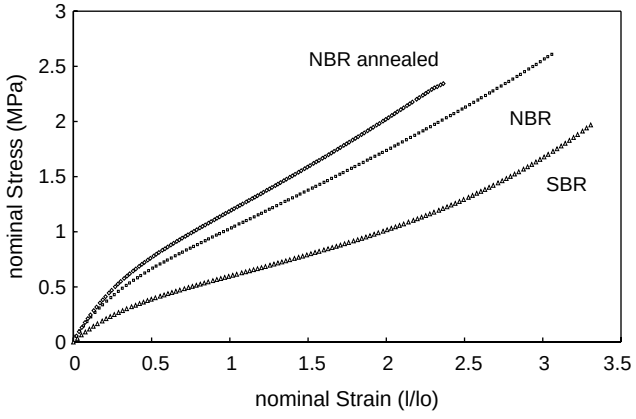

Fig. 3. Nominal stress versus nominal strain for SBR, NBR as received and annealed, at a strain rate of $0.4\ s^{-1}$ at room temperature.

Table 2
Determination of the variation of entropy induced by stretching on SBR and NBR as received and annealed in the framework of the basic assumptions of the gaussian statistical theory

Material	Density of active chain (mol cm^{-3})		λ	ΔS (mJ K^{-1} cm^{-3})
SBR	9.18×10^{-5}	As received	2.5	1.55
NBR	1.80×10^{-4}	As received	2.5	3.03
NBR	2.09×10^{-4}	Annealed	2	1.74

A link between elongation and conformational entropy modification can be achieved on the base of this model, considering the free energy function of the material:

$$F = U - TS$$

Finally, by neglecting the impact of internal energy contribution, one obtains for a uniaxial traction

$$\Delta S \approx \frac{nR}{2}\left(\lambda^2 + \frac{2}{\lambda} - 3\right)$$

with $n = \rho/M_c$ (mol·cm^{-3}).

We can roughly associate an imposed deformation to a variation of conformational entropy in the system (Table 2).

The value of elongation ratio corresponds to the maximal values allowed before rupture during stretching of the DMA samples. The variation of conformational entropy induced depends both on the degree of crosslinking of the material and on the elongation ratio. For two different microstructures (SBR and annealed NBR) we are able to obtain comparable variations of conformational entropy.

3.2. Effect of deformation on microstructure: WAXS measurements

It is known that amorphous polymers give rise to diffuse X-ray scattering. X-ray diffraction is of a great interest to explore the extent of medium range order in amorphous material. A modification of packing induces changes in the diffuse halo with a shift of the maximum along the q space axis and a variation of its width. A modification of the orientation induces an anisotropy of the spectrum, which splits into equatorial arcs [18]. We treat the problem considering successively these two features of the WAXS profile.

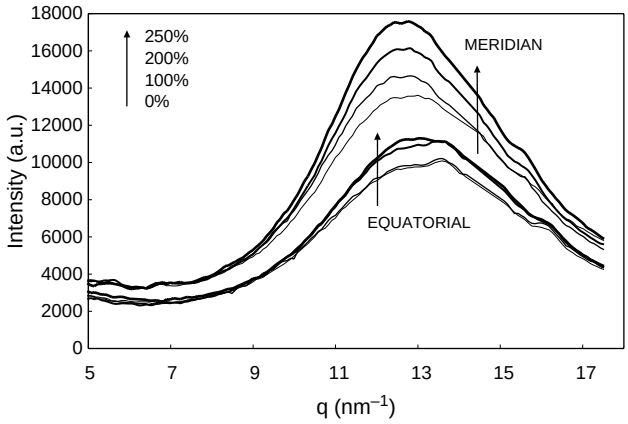

Fig. 4. Radial integration of the scattering spectra for the NBR in its as received state measured at various deformation ratios; equatorial and meridian scans.

We consider first the impact of deformation on the amorphous packing. Fig. 4 shows an example of a radial integration obtained from the scattering spectrum of the NBR in its as-received state, for various elongation ratios. On the figure we distinguish the equatorial and meridian scans both presented for ratios of deformation of 0, 100, 200 and 250%. The deformation has a weak effect on the amorphous halo for the meridian scan, whereas, one can observe a strong increase in the scattered intensity with elongation on the equatorial scan. The same observations can be done for all the materials investigated.

The Table 3 summarizes the results for the maximum peak position and the full width at half maximum (FWHM) obtained for each sample.

There is no shift of the peak maximum or variation in the width with the increase in the deformation. This observation implies that neither the deformation nor the annealing treatment (which modifies the density of crosslinking), have any significant impact on the amorphous density of the material, that means on the packing of the molecules. The result is not surprising when one considers that the material is not compressible above its glass transition temperature.

Secondly, the amorphous orientation is given by the azimuthal intensity variation in the amorphous halo, in the

Table 3
Results for the FWHM and peak position for the various materials studied (q in nm^{-1})

	SBR		NBR as recieved		NBR annealed	
	FWHM (q)	Peak position (q)	FWHM (q)	Peak position (q)	FWHM (q)	Peak position (q)
Equatorial integration (%)						
0	7.1	12.3	5	13	5.2	12.7
100	7.2	12.7	5.3	12.8	5.2	12.4
200	7.4	12	5	12.8	5.1	12.7
250	7.3	12.1	5.1	12.7		
Meridional integration (%)						
0	7	12.5	5.4	13	4.9	12.9
100	8	12.4	5.6	13.5	4.5	13.6
200	7.5	13	5.4	13.6	5.4	13.5
250	7.5	13	5.2	14.5		

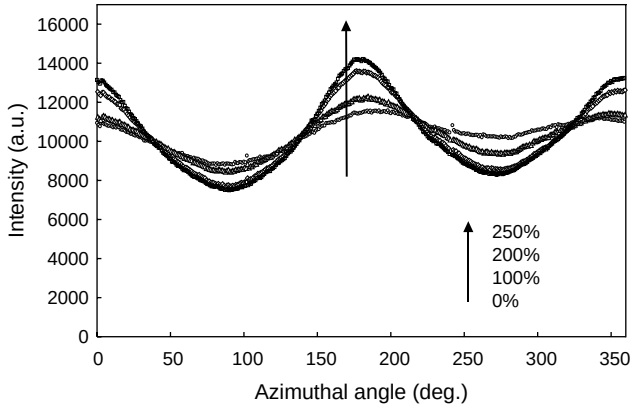

Fig. 5. Azimuthal integration of the 2D spectra for the SBR at elongation ratios of 0% (○), 100% (△), 200% (◇) and 250% (□).

form of an equatorial peak on a flat non-zero baseline. The equatorial amorphous scattering is due to segments parallel to the chain axis and the intensity below the baseline corresponds to the non-oriented isotropic amorphous component.

The Fig. 5 presents the azimuthal X-ray scattering intensity, i.e. the scattering intensity along the arc of an equatorial WAXS halo. The baseline is not completely flat for the non-stretched sample, which indicates an initial preferential orientation issued from the calendering of the elastomer sheet. The samples are stretched in the calendering direction. Qualitatively, it appears that stretching induces an increase in the initial preferential orientation, related to the increase in amplitude of the peak associated to diffusion of the amorphous oriented part of the material.

In a quantitative approach, it is possible to use the Herman's orientation factor that can be deduced according to [30]

$$f_{\mathrm{X-ray}} = \frac{1}{2}\left[3\frac{\int_0^{90} I(\Phi)\cos^2(\Phi)\sin(\Phi)\mathrm{d}\Phi}{\int_0^{90} I(\Phi)\sin(\Phi)\mathrm{d}\Phi} - 1\right]$$

where, $I(\Phi)$ is the scattered intensity, and Φ the azimuthal angle.

This expression is valid when the equatorial halo considered arises from intermolecular distances perpendicular to the direction of the polymer chain, which is reasonably the case here for a halo at a scattering angle 2θ around 18° (which gives a average period of 4.9 Å, using Bragg's law).

It should also be mentioned, that amorphous polymers give diffuse X-ray diffraction even in a perfectly oriented state due to intrinsic azimuthal width especially when the scattering segments are curved, as it is reminded by Van Aerle and Tol [30]. It implies that the experimental orientation factor $f_{\mathrm{X\text{-}ray}}$ is always smaller than the actual factor f. A correction of the underestimation is possible according to Pick's results [31], through the following expression:

$$f = K \cdot f_{\mathrm{X-ray}}$$

An intrinsic azimuthal width of 50° was roughly estimated, which corresponds to a correction factor of 3.5.

Table 4
Values of the Herman's orientation factor calculated from experimental data

$f=Kf_{\mathrm{X\text{-}ray}}$ (%)	SBR	NBR	NBR annealed
0	0.084	0.116	0.109
100	0.112	0.165	0.158
200	0.15	0.252	0.235
250	0.164	0.284	

The values of the Herman's orientation factor determined for all the materials are given in Table 4. The calculation of $f_{\mathrm{X\text{-}ray}}$ values is done on experimental data after the subtraction of the background X-ray scattering. In our case, the reference direction (imposing the 0° azimuthal angle) is taken parallel to the stretching direction. The scattering object being the intermolecular distance perpendicular to the main chain axis, it imposes that a perfectly oriented state of chain axis in the stretching direction will lead to a value of 1 for the Herman's orientation factor (a value of 0 corresponding to a perfectly isotropic material). The value of 1 is in fact never reached and all the more considering amorphous polymers, which present a very wide intrinsic azimuthal width.

The uniaxial deformation induces an increase of f for all the materials considered by a factor equal or larger than 2 for the larger deformation ratios investigated. This indicates a significant trend to alignment of the main chain axis. The reality of this trend is reinforced by the fact that the maximum elongation ratios obtained are the last that can be reached before rupture of the materials. If one considers the distribution of the lengths between crosslinks, a deformation close to the rupture of the sample implies that at least a fraction of the chains are severely extended and oriented.

As a conclusion, the WAXS measurements results confirm that uniaxial deformation does not lead to any modification of the density of packing, which is consistent with the value of the Poisson's coefficient of 0.5 above T_g, whereas a noticeable orientation of the macromolecules in the stretching direction is observed. This confirms the effect of deformation on the conformational entropy predicted by the statistical Gaussian theory for rubber elasticity.

4. Influence of deformation on molecular mobility

The first question to deal with is to define the most relevant parameter to check the mobility in our study. The DMA measurements give access to the complex modulus of the material

$$G^* = G' + iG''$$

where, G' is the storage modulus, and G'' the loss modulus.

In this part, the hypothesis is made that the modulus of the material is independent of the deformation state at the lowest temperature investigated for each experiment, i.e. in the glassy state. We normalise its value to unity at 90 K in order to improve the precision in the comparative discussion on molecular mobility. The ratio $G''/G' = \tan\delta$ is usually defined as the parameter which characterizes the molecular mobility.

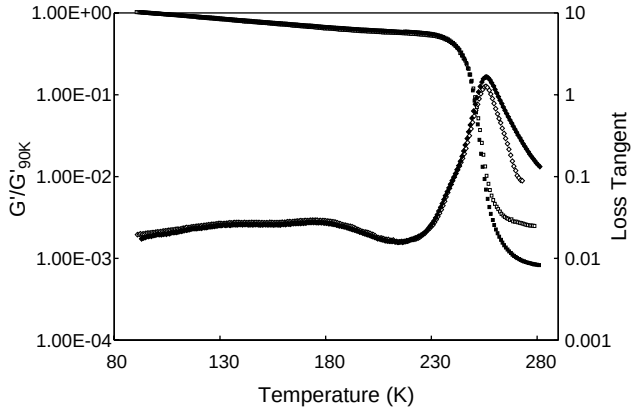

Fig. 6. Storage modulus G' and internal friction as a function of temperature for the NBR as received at deformation of 0% (■) and 200% (□).

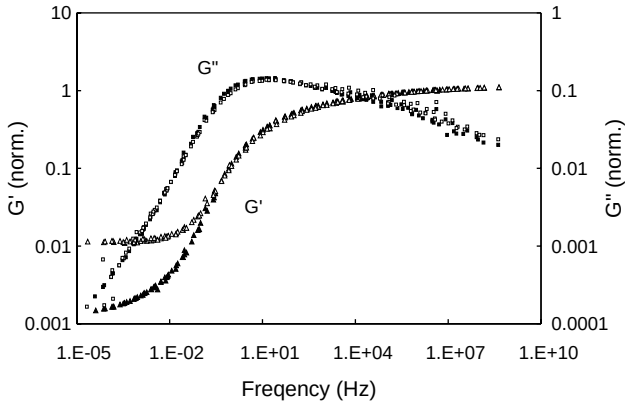

Fig. 8. G' ((□) 0% (■) 200%) and G'' ((△) 0% (▲) 200%) as a function of the frequency for NBR as received.

Let us take as a first example the results concerning the NBR in the as-received state. As shown on Fig. 6, above the main α-relaxation temperature, the storage modulus G' obtained in the rubbery state increases with the deformation. This can be easily explained by the statistical theory of rubber elasticity as a consequence of an alignment of the chain between the crosslinks without modification of the molecular mass between them. In turn, the increase affects the high temperature side of the internal friction peak as seen on Fig. 6. This effect has been interpreted in the past as a modification of the molecular mobility [20,21], whereas it is only the consequence of the storage modulus modification. This observation is confirmed by the results of the loss modulus G'' presented on Fig. 7 where no shift can be observed even for samples deformed at ratios of 200% (NBR) and 300% (SBR). Finally, the loss modulus G'' appears to be the only relevant parameter to characterize the mobility.

No shift along the temperature axis is observed under uniaxial deformation for materials with various microstructures and various crosslinking densities. These observations are valid for all deformation ratios investigated between 0 and 250%.

To confirm these results some experiments at various frequencies have been performed in order to build master curves around the main α transition. The master curves present the interest to test a possible influence of the frequency on the previous observations. They allow to describe the relaxation thanks to the shift factor $a(T)$ as a function of temperature and permit to test the thermo-rheological simplicity of the materials.

The master curves presented on Figs. 8–10 are obtained without any use of vertical shift, which indicates that the materials are thermo-rheologically simple in the range of frequencies investigated. The curves confirm the influence of the deformation on the storage modulus in the low frequency range and no shift is observable on the loss modulus curves in any case. The deformation has no impact on the molecular mobility in a very wide range of frequencies, whatever the microstructure and the cross-linking density are.

From the Arrhenius curves displaying $\log(\tau)$ as a function of $1000/T$ on the Fig. 11, it is possible to determine the various values of activation energy for both NBR and SBR. This Arrhenius curves are obtained by considering that $\omega\tau = 2\pi f\tau = 1$ (with f frequency in Hertz) at the main α-relaxation peak maximum. No significant change for the NBR with the annealing treatment is observed.

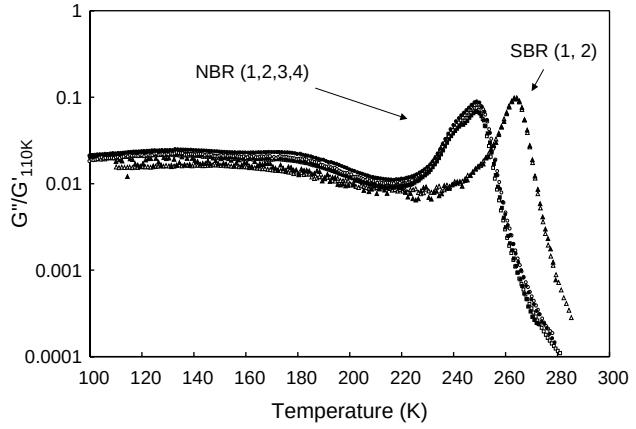

Fig. 7. Loss modulus G'' as a function of temperature for the NBR as received [1(□), 0%; 2(■), 250%], the NBR annealed [3(○), 0%; 4(●), 200%] and the SBR [1(△), 0%; 2(▲), 300%].

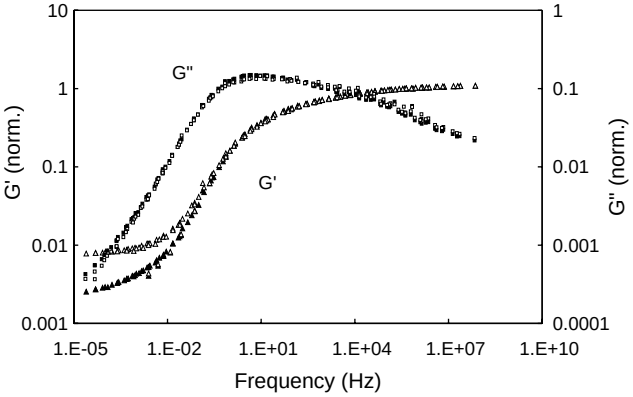

Fig. 9. G' ((□) 0% (■) 200%) and G''((△) 0% (▲) 200%) as a function of the frequency for NBR annealed.

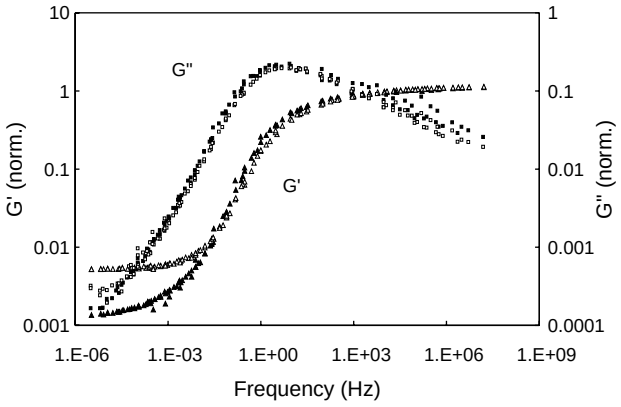

Fig. 10. G' ((□) 0% (■) 200%) and G'' ((△) 0% (▲) 200%) as a function of the frequency for SBR.

5. Discussion

Experimentally, it has been shown that a uniaxial elongation of crosslinked elastomers induces a modification of the orientation of the polymer chain but has no effect on the packing density of the system. These changes of the molecular structure have no impact on the molecular mobility of the system, independently of the chemical nature of the chain and the crosslinking density of the material.

In the literature, the effects of orientation in a polymer drawn below its glass transition temperature have been widely investigated leading to contradictory results. Spiess and co-workers have used ^{2}H NMR and ^{1}H NMR to study amorphous orientation in bisphenol-A polycarbonate specimens stretched below T_g. Their studies have shown that cold drawing leads to a partial immobilization of the phenyl mobility, attributed to a denser packing of the chains [23]. The evolution of the slow relaxation processes with the iso-configurational states obtained in deformed polymers ($T<T_g$) has also been widely studied with low frequency mechanical spectroscopy [2]. The sub-T_g relaxations characteristics are only weakly modified by deformation but the inelastic deformation induces a drastic increase in the mobility related to the low temperature side of the α process.

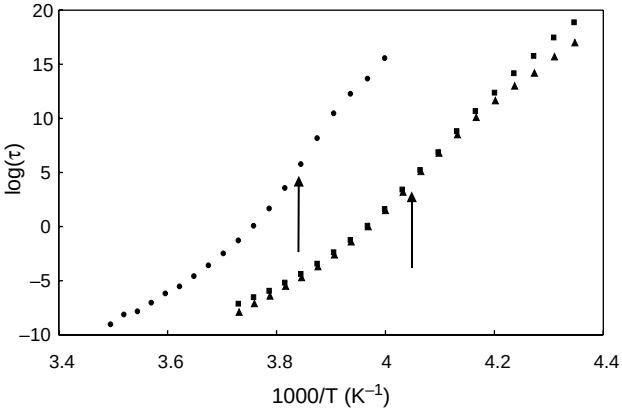

Fig. 11. Arrhenius plot presenting log(τ) versus 1000/T (NBR as received (■), NBR annealed (▲), SBR (●)), the arrows are representing the main α-transition temperature determined at 1 Hz.

On the contrary few studies address directly the effects of the orientation of the chain on the mobility when the polymer is stretched above the glass transition temperature T_g. Shelby et al. have investigated these effects via the evolution of aging parameters in bisphenol-A polycarbonate stretched above T_g and then cooled below T_g [24,25]. Volume relaxation rate and tensile creep measurements suggest that orientation induced by stretching in the rubbery state leads to a significant decrease in the α-relaxation's mobility while at the same time the movements associated to the β-relaxation become more mobile. The interpretation of these results is that the chain alignment leads to an increase of the cooperative domains related to the α process and to an increase of larger free volume holes in which individual segments associated to the β process can relax.

As far as DMA measurements are concerned, two examples are found in the literature. The first concerns Frosini and co-worker's works, which consist in damping measurements on samples stretched with a dead weight [26], which means that the constant deformation cannot be insured during cooling and during the increase in the modulus through T_g. They observed that the chain alignment as well as the removal of water lead to an increase in motion's energetical barriers, and a broadening of the relaxation times distribution.

In conditions much more similar to ours [21,20], Diaz Calleja and co-workers concluded to a shift towards low temperatures of the α-relaxation peak. They formulated an interpretation of their results on the base of the concept of compensation temperature. They argued in favor of a decrease in the number of visco-elastic mechanisms involved in the relaxation with the elongation. They introduce the idea of the compensatory character of an increase in the barrier opposed to Brownian motions and an increase in activation entropy as well as a decrease in conformational entropy.

As far as our experimental results are concerned, it should be emphasized that the use of a crosslinked material is the only way to maintain the entropic changes induced by stretching the material and to achieve an equilibrium state before quenching.

On one hand, WAXS measurements do not show any tighter chain packing induced by deformation. At a temperature above T_g, the material is supposed incompressible (Poisson coefficient of 0.5), and the free volume theory is applicable. If no variation of volume occurs, no modification of the molecular mobility is expected. The absence of variation in packing density has to be correlated to the rubber elasticity theory, already largely discussed in the literature, which deals with modifications of conformational entropy and enthalpy of an elastomeric system under elongation [7,19].

On the other hand, it has been shown that the deformation leads to a significant modification of the conformational entropy through chain orientation in the material. Considering the large-scale nature of the movements implied in the main α-relaxation, one could expect that a modification of the orientation of the chains has an impact on the α-relaxation's characteristics. WAXS experiments show that the Herman's orientation factor increases with deformation ratio. Moreover, since there is a large distribution of chains lengths between

crosslinks, one could expect that this factor represents an average value between slightly oriented and highly oriented zones. In spite of the existence of strongly oriented zones, no evolution of the α-peak features is observed (temperature, width, magnitude).

Consequently, we conclude that the alignment of the polymer chains induced by deformation, leading to a modification of the conformational entropy has no impact on the molecular mobility.

After these thermodynamic considerations, we are going to test if any link is possible between the conformational entropy and the activation entropy, and finally determine if the deformation has any impact on the activation parameters.

In the Starkweather formalism, a distinction is made between the pre-exponential factor, indicator of the activation entropy, related to the complexity of the relaxation, and the internal energy part related to energetic barriers opposed to molecular motions. A relation is found between activation enthalpy and activation entropy [10,11]

$$E_a = RT\left[1 + \ln\left(\frac{k}{2\pi h}\right) + \ln\left(\frac{T}{f}\right)\right] + T\Delta S_a$$

with $E_a = \Delta H_a + RT$.

The calculation of the activation energy of the relaxation gives access to the activation entropy, and allows to determine the degree of cooperativity of the relaxation. Following the argument developed by Starkweather [10], we are able to determine a value of activation entropy:

$$\Delta S_a = \frac{E_{a.exp} - E_{a.theo}}{T}$$

In this expression, $E_{a.exp}$ is the experimental activation energy determined from the Arrhenius plot and $E_{a.theo}$ is the theoretical activation energy described by Starkweather, considering an entropy of activation null for the relaxation considered

$$E_{a.theo} = RT(22.922 + \ln(T))$$

T being the temperature of the maximum of the loss modulus obtained at 1 Hz.

The different results concerning the entropy variations are compiled in Table 5. No comparison is possible between the results of activation entropy obtained by the Starkweather analysis, and the conformational entropy obtained using a simple form of the rubber elasticity theory.

Table 5
Synthesis of the results concerning the entropy of conformation and activation of the various materials

	$\Delta S_{activation}$ (kJ K^{-1} mol^{-1})	$\Delta S_{conformation}$ (J K^{-1} mol^{-1})	T_α at 1 Hz (K)
NBR as received	0.5	2.8×10^{-15}	249
NBR annealed	0.5	5.8×10^{-15}	249
SBR	0.7	3.3×10^{-15}	263

First, it appears that no direct connection between the conformational and the activation entropies can be done.

Then, the unreasonably high values of activation entropy are a symbol of the cooperative character of the α-relaxation. The values are of the same order of magnitude as those obtained elsewhere by Starkweather of 2 kJ K^{-1} mol^{-1} [22], but cannot be interpreted in a physical manner. The analysis of Starkweather gives only apparent values based on the hypothesis of microscopic independent movements. This assumption is not realistic as far as are concerned amorphous systems near their glass transition temperatures.

Finally, one can conclude that no effect of a uniaxial deformation is observed neither on the cooperativity of the main α transition, nor on the movements implied in this relaxation.

The Gibbs DiMarzio theory of the glass transition predicts a thermodynamic glass transition when the conformational entropy is zero [27]. From a conformational entropy standpoint, an oriented chain should have lower entropy that is why the effective glass transition of oriented samples should be raised. The motions associated to the α transition are associated to the glass transition of the elastomer. An increase in T_g as well as T_α with stretching ratio is indeed predicted by a modified form of the Gibbs-Di Marzio equation [28]:

$$\frac{T_{g(\lambda)}}{T_{g(\lambda=1)}} = \exp\left[\frac{G}{2\Delta C_p T_0}(\lambda^2 + 2\lambda - 3)\right]$$

where, λ is the uniaxial stretch ratio; G is the shear modulus at test temperature T_0 and ΔC_p is the heat capacity difference between the liquid and the glassy states.

Our data does not compare well with this model but molecular dynamics simulations performed on oriented styrene–butadiene rubber chains may provide insights in these discrepancies [29]. They give a better understanding of the molecular changes taking place during stretching in an oriented elastomer, and how these changes may affect the relaxation processes. It is generally accepted that the microstructural changes with chain orientation can be separated into two components. The first one is due to changes in the inter-molecular interactions and the second one is brought about by the changes in intra-molecular potential energy. Our molecular simulations suggest that the inter-molecular interactions are not significantly modified in the stretched network. This result could explain why the time and temperature dependences of the large-scale relaxation processes are not much changed in the oriented samples. On the contrary, orientation and stiffening of the chain significantly influence intra-molecular interactions. Short range vibrational motions are enhanced by chain alignment and shifted to higher frequencies since the effective vibrational spring constant increases. Mermet et al. have indeed observed with low frequency Raman scattering [1] an enhanced mobility in the high frequency range for polymers stretched around T_g.

6. Conclusion

The uniaxial deformation performed above T_g on NBR with two different crosslinking densities and SBR, leads to a modification of the arrangement of the chain. This has been detected by mechanical testing, considerations based on the statistical theory of rubber elasticity and WAXS measurements. The modification of conformational entropy in the equilibrium state can be frozen through the main α transition to temperature below the secondary β process thanks to the reticulation of the materials. Considering the right indicator of molecular mobility (G''), it has been demonstrated that a modification in conformational entropy has no effect on molecular mobility. In addition it appears that a clear distinction has to be done between the thermodynamical conformational entropy, and the relaxation activation entropy. Finally, our observations, and their apparent contradiction with the Gibbs Di Marzio theory, should find explanations thanks to studies at a more local scale by considering the impact of chain conformation, respectively, on intra-molecular and inter-molecular interactions.

Acknowledgements

The authors gratefully acknowledge L. Guerbé from Paulstra (France), and J. Ramier for providing the materials.

References

[1] Mermet A, Duval E, Etienne S, G'Sell C. J Non-Cryst Solids 1996;196:227.
[2] Gauthier C, Pelletier J-M, David L, Vigier G, Perez J. J Non-Cryst Solids 2000;274:181.
[3] Roland CM, Ngai KL, Plazek DJ. Comput Theor Polym Sci 1997;7(3):133.
[4] Oleynik E. Prog Colloid Polym Sci 1989;80:140.
[5] Sperling LH. Introduction to physical polymer science. 2nd ed. New York: Wiley; 1992.
[6] Shen M. Macromolecules 1969;2(4):358.
[7] Lyon RE, Farris RJ. Polymer 1987;28:1127–32.
[8] Moshin MA, Treloar LRG. Polymer 1987;28:1893.
[9] Frosini V, Woodward AE. J Polym Sci, Part: A-2 1969;7:525.
[10] Starkweather Jr HW. Polymer 1991;32(13):2443.
[11] Starkweather Jr. HW. Macromolecules 1981;14:1277.
[12] Diaz-Calleja R, Riande E, Guzman J. J Polym Sci, Part B: Polym Phys 1990;28:1551.
[13] Diaz-Calleja R, Riande E, Guzman J. Polymer 1987;28:2190.
[14] Etienne S, Cavaillé J-Y, Perez J, Point R, Salvia M. Rev Sci Instrum 1982;53:1231.
[15] Brandrup J, Immergut EH, Grulke EA. Polymer handbook. 4th ed. Wiley; 1999 p. V-2.
[16] Sperling LH. Introduction to physical polymer science. 2nd ed. New York: Wiley; 1992 p. 429.
[17] De Gennes PG. Scaling concepts in polymer physics. Ithaca, NY: Cornell University Press; 1979.
[18] Murthy NS, Minor H, Bednarczyk C, Krimm S. Macromolecules 1993;26:1712–21.
[19] Godovsky YK. Polymer 1981;22:75.
[20] Diaz-Calleja R, Riande E, Guzman J. Polymer 1988;29:2203.
[21] Diaz-Calleja R, Riande E, Guzman J. J Polym Sci 1986;24:337.
[22] Starkweather Jr HH. Macromolecules 1991;23:328.
[23] Weigand F, Spiess HW. Macromolecules 1995;28:6361.
[24] Shelby MD, Hill AJ, Burgar MI, Wilkes GL. J Polym Sci, Part B: Polym Phys 2001;39:32.
[25] Shelby MD, Wilkes GL. Polymer 1998;39:6767.
[26] Frosini V, Woodward AE. J Polym Sci, Part: A-2 1969;7:525.
[27] DiMarzio AEA. J Res Natl Bur Stand, Sect A 1964;68A:611.
[28] Shelby MD, Wilkes GL. J Polym Sci, Part B: Polym Phys 1998;36:2111.
[29] Munch E, Sixou B, Pelletier J-M, Vigier G. Molecular Simulation, in preparation.
[30] Van Aerle NAJM, Tol JW. Macromolecules 1994;27:6520–6.
[31] Pick M, Lovell R, Windle AH. Polymer 1980;21:1017–24.